*Journal of Inclusion Phenomena and Molecular Recognition in Chemistry* **15:** 385–398, 1993.



# Helical Tubulate Inclusion Compounds of Ferrocene and Squalene

ALISON T. UNG, ROGER BISHOP,* DONALD C. CRAIG, IAN G. DANCE, A. DAVID RAE and MARCIA L. SCUDDER
*School of Chemistry, The University of New South Wales, Kensington, N.S.W. 2033, Australia.*

(Received: 1 June 1993)

**Abstract.** The inclusion compounds of 2,8-dimethyltricyclo[5.3.1.$1^{3,9}$]dodecane-*syn*-2,*syn*-8-diol, **3**, with ferrocene and with squalene have been prepared. The crystal structures of these helical tubulate compounds: $(\mathbf{3})_3\cdot(\text{ferrocene})_{0.75}$ [$P3_121$, $a = b = 13.7480(6)$, $c = 7.0312(5)$ Å, $Z = 1$, $R = 0.038$] and $(\mathbf{3})_3\cdot(\text{squalene})_{0.23}$ [$P3_121$, $a = b = 13.677(1)$, $c = 7.0533(9)$ Å, $Z = 1$, $R = 0.042$] are described.

**Supplementary Data** relating to this article are deposited with the British Library as supplementary publication No. SUP 82151 (16 pages).

**Key words:** Hydrogen bonding, alicyclic diol, helical tubulate, crystal structure, ferrocene, squalene.

## 1. Introduction

The helical tubuland hosts are a series of alicyclic diols which crystallise with a hydrogen-bonded lattice containing parallel helical canals which trap guest molecules. In developing this family of substances we have sought to synthesise helical tubuland diols which would provide a range of different canal dimensions and thus which would have a gradation of inclusion properties [1, 2]. Recently we have reported preliminary structural details of typical helical tubulate inclusion compounds formed by diols **1** [3] and **2** [4] (See Figure 1).

2,8-Dimethyltricyclo[5.3.1.$1^{3,9}$]dodecane-*syn*-2,*syn*-8-diol, **3** has the largest unobstructed canal cross-sectional area of the first five helical tubuland diols [5–7]. Figure 2 shows a slice through the needle axis of crystalline **3** showing the star-shaped cross-sectional area (*ca.* 34.7 Å$^2$) of its parallel canals. It should be pointed out that this cross-section is akin to the view looking along an indented pipe. Therefore additional space for guests is available in indentations along the canals. The helical characteristics of the canals are also lost in such a projection. The considerable volume available suggested that **3** should be capable of including much larger guests than those encountered earlier [3, 4]. This was found to be correct and we here report on the structures of the helical tubulates of

* Author for correspondence.

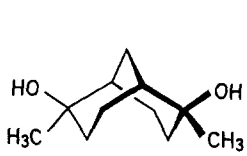


1

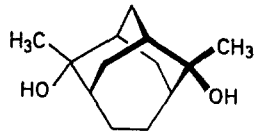


2

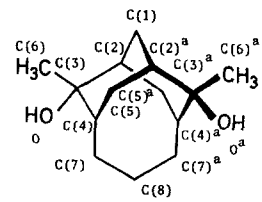


3

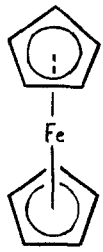


4

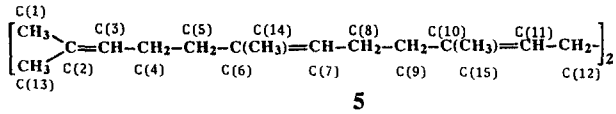


5

Fig. 1. Structures of diols **1–3**, ferrocene **4** and squalene **5**. The crystallographic numbering systems used for the structures involving **3** and **5** are indicated.

diol **3** with ferrocene **4**, and with the biologically significant triterpene squalene (2,6,10,15,19,23-hexamethyl-2,6,10,14,18,22-tetracosahexaene) **5**.

## 2. Experimental

### 2.1. PREPARATIVE WORK

Melting points were determined on a Kofler instrument and are uncorrected. $^1$H NMR data were recorded with a Bruker AC300 instrument (300 MHz) and are reported as chemical shifts ($\delta$) relative to tetramethylsilane. The IR spectra were recorded on a Hitachi 260-10 spectrophotometer. Elemental analyses were carried out at the University of New South Wales by Dr. H. P. Pham. Powder diffraction data were recorded using a Siemens D500 instrument, and confirmed the presence of the helical tubuland host lattice by comparison with previous examples.

#### 2.1.1. *(2,8-Dimethyltricyclo[5.3.1.1$^{3,9}$]dodecane*-syn-2,syn-*8-diol* **3**) – *(Ferrocene* **4**) *Inclusion Compound*

Diol **3** [5] (0.05 g, 0.223 mmol) was dissolved upon warming in a saturated solution of ferrocene **4**, in acetonitrile (2 mL). The solution was left to stand at room temperature with slow evaporation. Orange-yellow needle-like crystals were obtained, m.p. 119–120°C, which were stable at room temperature and suitable for X-ray analysis.

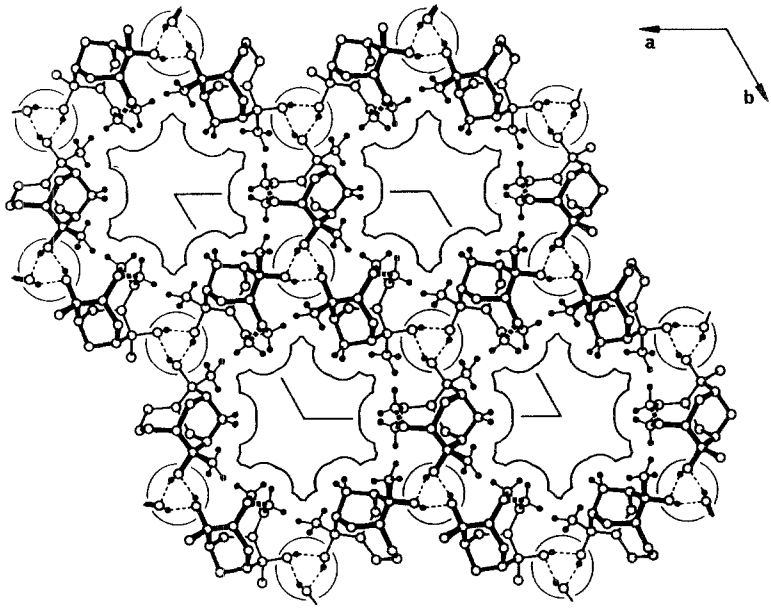


Fig. 2. Projection view in the *ab* plane of the diol **3** lattice. Selected hydrogen atoms (filled circles) with their van der Waals radii define the star-shaped canal cross-sections of the host network. The hydrogen bonded spines are circled and hydrogen bonds are represented as dashed lines.

$\nu_{max}$ (paraffin mull) 1100 and 825 $cm^{-1}$ and $^1H$ NMR $\delta$ ($CDCl_3$) 4.27 (ferrocene guest peaks only); NMR integration indicated the composition $(\mathbf{3})_3 \cdot (\text{ferrocene})_{0.71}$. [Found: C, 73.30; H, 9.82. $(C_{14}H_{24}O_2)_3 \cdot (C_{10}H_{10}Fe)_{0.71}$ requires C, 73.25; H, 9.90%].

### 2.1.2. *(2,8-Dimethyltricyclo[5.3.1.1$^{3,9}$]dodecane*-syn-*2,*syn-*8-diol* **3***) – (Squalene* **5***) Inclusion Compound*

Diol **3** [5] was slightly soluble in neat squalene **5**. Unsolvated diol was dissolved upon warming in squalene (5 mL) and the solution allowed to cool to room temperature and stand overnight. The fine, needle-like crystals were filtered, m.p. 127–128°C. $^1H$ NMR $\delta$ 1.61 and 5.10 (squalene guest peaks only); NMR integration indicated the composition $(\mathbf{3})_3 \cdot (\text{squalene})_{0.21}$. [Found: C, 75.60; H, 11.13. $(C_{14}H_{24}O_2)_3 \cdot (C_{30}H_{50})_{0.21}$ requires C, 76.40; H, 10.95%]. Crystals suitable for X-ray structural work were prepared by allowing crystals to grow from a solution of diol **3** (0.05 g) in squalene (5 mL) and mesitylene (2 mL).

TABLE I. Numerical details of the solution and refinement of structures $(\mathbf{3})_3 \cdot (\text{ferrocene})_{0.75}$ and $(\mathbf{3})_3 \cdot (\text{squalene})_{0.23}$

| | | |
|---|---|---|
| Formula | $(C_{14}H_{24}O_2)_3 \cdot (FeC_{10}H_{10})_{0.75}$ | $(C_{14}H_{24}O_2)_3 \cdot (C_{30}H_{50})_{0.23}$ |
| Formula mass | 812.6 | 767.5 |
| Crystal description | {100}{010}{001}{1-10} | {100}{010}{1-10}(00-1)(-111) |
| Space group | $P3_121$ | $P3_121$ |
| $a, b$/Å | 13.7480(6) | 13.677(1) |
| $c$/Å | 7.0312(5) | 7.0533(9) |
| $V$/Å$^3$ | 1150.91(9) | 1142.6(2) |
| Temp./°C | 21(1) | 21(1) |
| $Z$ | 1 | 1 |
| $D_{calc.}$/g cm$^{-3}$ | 1.17 | 1.12 |
| Radiation, $\lambda$/Å | Cu$K_\alpha$, 1.5418 | Cu$K_\alpha$, 1.5418 |
| $\mu$/cm$^{-1}$ | 23.58 | 5.19 |
| Crystal dimensions/mm | 0.13 × 0.16 × 0.34 | 0.11 × 0.12 × 0.30 |
| Scan mode | $\theta/2\theta$ | $\theta/2\theta$ |
| $2\theta_{max}$/deg. | 120 | 140 |
| $\omega$ scan angle | 0.60 + 0.15 tan $\theta$ | 0.60 + 0.15 tan $\theta$ |
| No. of intensity measurements | 3391 | 4318 |
| Criterion for observed reflection | $I/\sigma(I) > 3$ | $I/\sigma(I) > 3$ |
| No. of independent obsd reflections | 1026 | 1283 |
| No. of reflections ($m$) and variables ($n$) in final refinement | 1026, 141 | 1283, 127 |
| $R = \Sigma^m \lvert\Delta F\rvert / \Sigma^m \lvert F_0\rvert$ | 0.038 | 0.042 |
| $R_w = [\Sigma^m w \lvert\Delta F\rvert^2 / \Sigma^m w \lvert F_0\rvert^2]^{1/2}$ | 0.047 | 0.048 |
| $s = [\Sigma^m w \lvert\Delta F\rvert^2 / (m-n)]^{1/2}$ | 2.47 | 1.90 |
| Crystal decay | none | none |
| Max., min. transmission coefficients | 0.76, 0.49 | 0.95, 0.86 |
| $R$ for multiple measurements (no.) | 0.033, 2989 | 0.036, 3614 |

## 2.2. X-RAY DATA COLLECTION, PROCESSING, AND REFINEMENT FOR THE DIOL **3** – FERROCENE INCLUSION COMPOUND

Data for both structures were recorded using an Enraf Nonius CAD4 X-ray diffractometer. Numerical details pertaining to the collection of data, data processing and solution of the structures are given in Table I. Procedures adopted for data collection and processing have been described [8].

For the ferrocene inclusion compound the published positional parameters for the diol **3** were used as input for the initial Fourier calculations [5]. A Fourier map indicated the position of the Fe atom of the ferrocene. There were a few other small peaks at appropriate distances from the Fe atom to be carbon atoms of the cyclopentadienyl rings, however, it was not possible to locate all ten carbon atoms. This was because of the imposed symmetry of the host lattice in these calculations requiring sixfold disordering of guest molecules in the centre of the

canal (see Results and Discussion section). Coordinates for a published structure of ferrocene were therefore used [9] which were fitted to the observed peaks. Refinement was continued with program RAELS [10] with rigid group and slack constraint capabilities. The coordinates of each atom of the ferrocene molecule were allowed to vary, but with slack constraints maintaining reasonable geometry. Hydrogen atoms of the guest were included in calculated positions. The Fe atom was refined with anisotropic thermal parameters and the remainder of the ferrocene molecule was assigned a 15 parameter *TLX* thermal mode (where $T$ is the translation tensor, $L$ is the libration tensor and $X$ is the origin of libration, initially fixed on the Fe atom). The atoms of the host diol were refined anisotropically in the usual way. Refinement converged with $R = 0.038$ (with that for data with $\sin\theta/\lambda < 0.1$ 0.159). The hydroxy hydrogen atom was included in its map position and its position was refined. All other hydrogen atoms of the host were included in calculated positions and were not refined; all hydrogen atoms were assigned isotropic temperature factors equivalent to those of the atoms to which they were bound. The occupancy of the ferrocene molecule, which had initially been set to 0.1667 (one ferrocene molecule per unit cell length), refined to a value of 0.128. It was therefore set to 0.125, which corresponds to three ferrocene molecules fitting within four unit cell lengths. This gives an average Fe–Fe distance of $4c/3 = 9.37$ Å. The actual Fe–Fe distances range from 9.24 to 9.56 Å. The shortest inter-ferrocene C–C distance is 5.26 Åwhich is somewhat longer than seems necessary, but is too short to consider the existence of a co-guest such as acetonitrile from which the crystals were grown. The shortest ferrocene-host distance was 3.58 Å, between atoms C(51) and C(8). Since ferrocene has a significant imaginary component to its anomalous scattering, it is possible to discriminate between the structure in $P3_121$ and its mirror image in $P3_221$. $R$ for the second alternative was 0.080, clearly indicating that the correct enantiomer had been chosen initially. $R$ for the host structure alone was 0.187 (with that for the five reflections with $\sin\theta/\lambda < 0.1$ which are most sensitive to omitted electron density, 0.51). The largest peak in the final difference map was 0.25 e $\text{Å}^{-3}$.

### 2.3. X-RAY DATA COLLECTION, PROCESSING, AND REFINEMENT FOR THE DIOL **3** – SQUALENE INCLUSION COMPOUND

The published positional parameters [5] for the diol were used as input for the initial Fourier calculations. However, it was not possible to model the residual electron density observed along the canal, since this represented a sixfold disorder of a molecule containing 30 carbon atoms. The determination of a model for the guest squalene molecule was carried out initially by molecular modelling using the program InsightII [11]. A molecule of squalene was constructed, but there were clearly a very large number of conformations which the molecule could adopt depending on the values of the torsion angles along it. Three previous X-ray structure analyses have been carried out on squalene [12–14]. Torsion angles from

the -110°C study [13], as quoted by MacNicol [14], were modified to give values of exactly 60, 120 or 180° as an initial model for the guest. The resulting molecule when viewed from one end appeared as a compact molecule with a triangular cross section, an ideal arrangement to occupy the helical tubuland canal. Determination of the structure was continued crystallographically using RAELS [10]. Firstly the centre of the central bond of the squalene molecule was positioned on one of the two-fold axes in the unit cell, so that only half of the squalene molecule need be refined. Then all the various options for location, orientation and enantiomer (with regard to the handedness of the molecular spiral) for the guest molecule as a rigid group were systematically refined. Consideration was taken of both the $R$ factors and resulting contacts with the walls of the canal. The starting point selected for the final refinement gave $R = 0.054$ and the shortest guest-host interactions *ca.* 3 Å. The position of each carbon atom of the asymmetric unit of the guest was refined. Slack constraints were used to maintain sensible bond lengths and angles for the guest and to keep torsion angles about the double bonds at 180°. Initially the occupancy was fixed at 0.071 – the ratio of squalene : diol per asymmetric unit as determined from NMR experiments. Hydrogen atoms of the guest were included in calculated positions. A single isotropic thermal parameter was used for all atoms of the guest molecule. When refinement had converged, packing between squalene molecules was considered, and it was found that with an occupancy of 0.077 it was possible to accommodate squalene molecules end to end with the closest squalene-squalene distance being 4.7 Å. This value was incorporated into the refinement, with improvement in the $R$ factor. The atoms of the host diol were refined anisotropically in the usual way. Refinement converged with $R = 0.042$ (with that for data with $\sin\theta/\lambda < 0.1$ 0.075). The hydroxy hydrogen atom was included in its map position and its position was refined. All other hydrogen atoms of the host were included in calculated positions and were not refined; all hydrogen atoms were assigned isotropic temperature factors equivalent to those of the atoms to which they were bound. $R$ for the host structure alone was 0.058 (with that for the 6 reflections with $\sin\theta/\lambda < 0.1$ which are most sensitive to omitted electron density, 0.31). The largest peak in the final difference map was 0.20 e $\text{Å}^{-3}$.

## 3. Results and Discussion

A significant difficulty in performing single crystal X-ray studies of many multi-molecular inclusion systems, including the helical tubulates, is the incommensurate symmetry of the host and guest components. There is no strict requirement for stoichiometry between host and guest, although it may be present. In the case of the helical tubuland structure such problems are further compounded by disorder of the guest within the ordered host lattice. For space group $P3_121$ the central portion of the canal (near $x = y = 0$), where the guest molecules lie, is an intersection of the threefold screw axis and twofold axes perpendicular to it $c/6$ (*ca.* 1.2 Å) apart. No guest molecule could conform to this symmetry. When the guest molecule

is subject to such sixfold disorder it becomes difficult to locate individual atoms crystallographically, especially when they are atoms of low atomic number such as carbon.

The original benzene inclusion compound of **3** was refined to give a structure factor residual $R$ of 0.038 without consideration of the guest molecules in the refinement of the structure [5], although other evidence indicated a composition of approximately $(\mathbf{3})_3 \cdot (C_6H_6)$. Thus the conventional residual $R$ may be quite low, even though part of the structure has been omitted. A much better indicator is $R$ for the very low angle data. This is particularly sensitive to omitted electron density and so $R$ for data with $\sin\theta/\lambda < 0.1$ was continually monitored while refining these structures.

Such considerations are the reason why it was especially useful to use published coordinates (for ferrocene) or published torsional angles in a computed model (for squalene) as starting models for the refinement of the structure determinations published here. Refinement of structures with such disorder would be impossible without a program [10] capable of rigid grouping and slack constraints.

Details of the solution and refinement of the diol **3** – ferrocene inclusion compound are presented in Table I. Fractional coordinates for the non-hydrogen atoms are listed in Table II; bond lengths and angles for **3** are given in Table III and those for ferrocene in Table IV. Figure 1 shows the crystallographic numbering system employed for **3**. A projection view of the host-guest arrangement as a slice across one canal only of the lattice is shown in space filling representation in Figure 3. This reveals the guest to be tilted at an angle of approximately 66° to the canal axis. There appears to be a significant volume of space still available across the star-shaped canal area suggesting that it may prove possible to enclose guest molecules with an even larger cross-section.

X-ray [9, 15, 16] and neutron [17] diffraction studies of solid ferrocene indicate that neither the eclipsed $(D_{5h})$ nor staggered $(D_{5d})$ ring conformations are adopted. Rather an arrangement is preferred with a ring rotation of *ca.* 10° from the fully eclipsed conformation. The structure found here, and shown in space filling representation by Figure 3, has the cyclopentadienyl rings rotated by some 3° from each other, although little confidence can be placed in their exact orientations because of disorder and the refinement problems noted earlier.

Ferrocene has previously been reported as a guest species trapped within a variety of host lattices, notably: (thiourea)$_3$·(**4**) [18–20], ($\alpha$-cyclodextrin)$_2$·(**4**) [21, 22], ($\beta$-cyclodextrin)·(**4**) [21, 23], ($\gamma$-cyclodextrin)·(**4**) [21], and (deoxycholic acid)$_2$·(**4**) [24]. Similar problems of refinement were encountered in most of those investigations which examined these materials by X-ray crystallography [18, 20, 24]. ($\alpha$-Cyclodextrin)$_2$·(**4**) was found to have the ferrocene cyclopentadienyl rings rotated from the eclipsed position by *ca.* 30°, possibly due to the influence of the twofold symmetry of the hydrophobic cavity [22].

Details of the solution and refinement of the diol **3** – squalene inclusion compound are also presented in Table I. Fractional coordinates for the non-hydrogen

TABLE II. Fractional coordinates for the non-hydrogen atoms of $(\mathbf{3})_3 \cdot (\text{ferrocene})_{0.75}$.

| | $x$ | $y$ | $z$ |
|---|---|---|---|
| O | -0.2363(1) | 0.3798(2) | 0.2226(2) |
| C(1) | 0.0000 | 0.3208(4) | 0.1667 |
| C(2) | -0.0987(2) | 0.3365(2) | 0.1135(3) |
| C(3) | -0.1422(2) | 0.3685(2) | 0.2879(3) |
| C(4) | -0.0503(2) | 0.4759(2) | 0.3893(3) |
| C(5) | 0.0640(2) | 0.4801(2) | 0.3943(3) |
| C(6) | -0.1901(2) | 0.2716(2) | 0.4323(3) |
| C(7) | -0.0436(2) | 0.5872(2) | 0.3336(4) |
| C(8) | -0.0472(4) | 0.6188(4) | 0.1486(8) |
| HO | -0.2636(28) | 0.3922(31) | 0.3101(43) |
| Fe | -0.0020(11) | -0.0291(6) | 0.1783(24) |
| C(11) | 0.1278(15) | -0.0290(15) | 0.3212(26) |
| C(21) | 0.0227(20) | -0.0979(16) | 0.4188(26) |
| C(31) | -0.0331(19) | -0.0354(12) | 0.4642(26) |
| C(41) | 0.0413(14) | 0.0789(11) | 0.4040(26) |
| C(51) | 0.1395(13) | 0.0815(13) | 0.3243(25) |
| C(12) | 0.0254(12) | -0.0758(10) | -0.0839(26) |
| C(22) | -0.0889(10) | -0.1497(12) | -0.0229(30) |
| C(32) | -0.1484(11) | -0.0914(18) | 0.0268(35) |
| C(42) | -0.0731(18) | 0.0249(17) | -0.0210(33) |
| C(52) | 0.0276(17) | 0.0303(15) | -0.0951(28) |

atoms are listed in Table V; bond lengths and angles for **3** are given in Table III and those for squalene in Table VI. In both structures, the propano bridge of the diol C(8) atom was disordered as required by space group symmetry. Refinement gave unequal C(7)–C(8) and C(7)$^a$–C(8) lengths, one being too short for a normal C–C and one being too long. In addition, the C(7)–C(8)–C(7)$^a$ angle was larger than expected for a normal, tetrahedral C(8) atom. This implies some uncertainty in the position of C(8) which is reflected in the higher standard deviation associated with it. The same phenomenon has been observed in the refinement of the host with benzene [5], and of its double epimer in the same helical tubuland lattice [25].

Figure 1 indicates the crystallographic numbering system used for squalene. The arrangement of a guest molecule within one canal of the helical tubulate inclusion compound is illustrated in space filling representation in Figures 4 and 5. The former figure shows a slice across one canal of the lattice with the squalene packed tightly within while the latter figure shows a side view of the same arrangement. In this diagram, one column of diol molecules has been removed to expose the worm-like guest molecule threaded through the host canal.

TABLE III. Dimensions of diol **3** in $(\mathbf{3})_3$·(ferrocene)$_{0.75}$ and $(\mathbf{3})_3$·(squalene)$_{0.23}$.

| | $(\mathbf{3})_3$·(ferrocene)$_{0.75}$ | $(\mathbf{3})_3$·(squalene)$_{0.23}$ |
|---|---|---|
| *Bond Lengths* (Å) | | |
| O–C(3) | 1.452(3) | 1.449(2) |
| C(1)–C(2) | 1.523(2) | 1.527(2) |
| C(2)–C(3) | 1.523(3) | 1.539(2) |
| C(2)–C(5)[a] | 1.551(3) | 1.537(2) |
| C(3)–C(4) | 1.555(3) | 1.547(2) |
| C(3)–C(6) | 1.536(3) | 1.537(3) |
| C(4)–C(5) | 1.544(3) | 1.551(3) |
| C(4)–C(7) | 1.537(4) | 1.533(3) |
| C(7)–C(8) | 1.380(6) | 1.382(5) |
| C(7)[a]–C(8) | 1.574(6) | 1.581(6) |
| O–HO | 0.78(3) | 0.93(2) |
| *Bond Angles* (°) | | |
| C(2)–C(1)–C(2)[a] | 108.1(3) | 107.7(2) |
| C(1)–C(2)–C(3) | 110.4(2) | 110.1(1) |
| C(1)–C(2)–C(5)[a] | 108.2(2) | 108.5(1) |
| C(3)–C(2)–C(5)[a] | 117.4(2) | 117.6(1) |
| C(2)–C(3)–O | 106.0(2) | 105.6(1) |
| C(2)–C(3)–C(4) | 113.2(2) | 112.9(1) |
| C(2)–C(3)–C(6) | 110.0(2) | 109.8(1) |
| O–C(3)–C(4) | 112.8(2) | 113.0(1) |
| O–C(3)–C(6) | 106.5(2) | 106.3(1) |
| C(4)–C(3)–C(6) | 108.2(2) | 109.0(1) |
| C(3)–C(4)–C(5) | 112.0(2) | 111.8(1) |
| C(3)–C(4)–C(7) | 116.4(2) | 116.7(1) |
| C(5)–C(4)–C(7) | 114.5(2) | 114.7(2) |
| C(4)–C(5)–C(2)[a] | 118.5(2) | 118.6(1) |
| C(4)–C(7)–C(8) | 124.0(3) | 124.1(2) |
| C(7)–C(8)–C(7)[a] | 120.6(4) | 120.2(3) |
| C(3)–O–HO | 109(1) | 107(1) |

[a] $-x, -x + y, 1/3 - z$.

Squalene has previously been included within the hexa-host molecule hexakis (4-*t*-butylphenylthiomethyl)benzene and found by MacNicol *et al.* [14] to have a significantly altered conformation from that determined from low-temperature X-ray studies on solid squalene [13]. After refinement, the torsion angles (Table VI) determined in our study had changed markedly from the initial values used and were different again from those found in the previous studies (except those about

TABLE IV. Ferrocene dimensions in $(\mathbf{3})_3 \cdot (\text{ferrocene})_{0.75}$.

| | | | |
|---|---|---|---|
| Fe–C and C–C distances (Å) were slack constrained in refinement to be equal. | | | |
| Fe–C | 2.048(4) | | |
| C–C | 1.445(5) | | |
| *Bond Angles* (°) | | | |
| C(51)–C(11)–C(21) | 103.4(7) | C(11)–C(21)–C(31) | 111.7(7) |
| C(21)–C(31)–C(41) | 106.5(7) | C(31)–C(41)–C(51) | 106.6(7) |
| C(41)–C(51)–C(11) | 111.6(6) | C(52)–C(12)–C(22) | 101.1(9) |
| C(12)–C(22)–C(32) | 113.6(6) | C(22)–C(32)–C(42) | 105.4(5) |
| C(32)–C(42)–C(52) | 106.2(7) | C(42)–C(52)–C(12) | 113.1(8) |

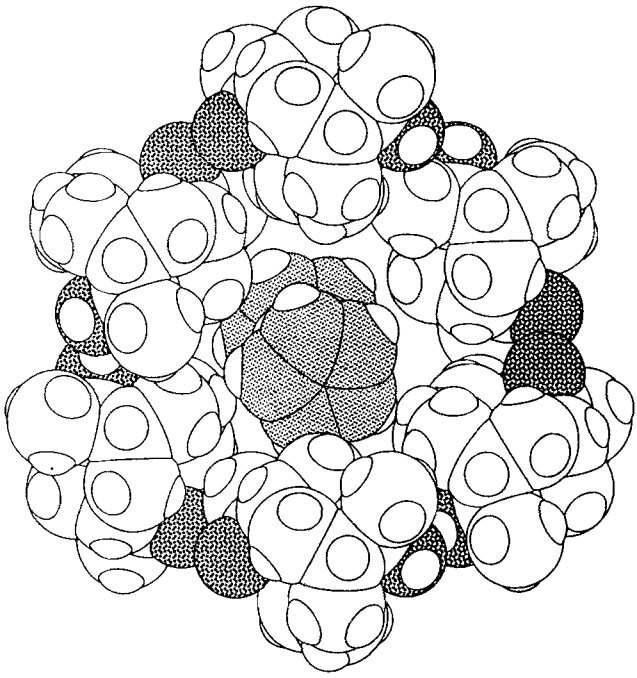

Fig. 3. View along one canal of the helical tubulate inclusion compund $(\mathbf{3})_3 \cdot (\text{ferrocene})_{0.75}$ showing the tilted orientation of the guest. Ferrocene carbon atoms are emphasised using light stippling; heavy stippling indicates the oxygen atoms present in the host molecules.

the double bonds which were all near 180°). Squalene is clearly able to adopt a myriad of different conformations. In this case the one adopted resulted in a long chain roughly triangular in cross section which fitted snugly within the canal.

In previous work on helical tubulate inclusion compounds of diol **1** we noted [3] that the $a(= b)$ dimension of the host lattice has a significant elasticity such that

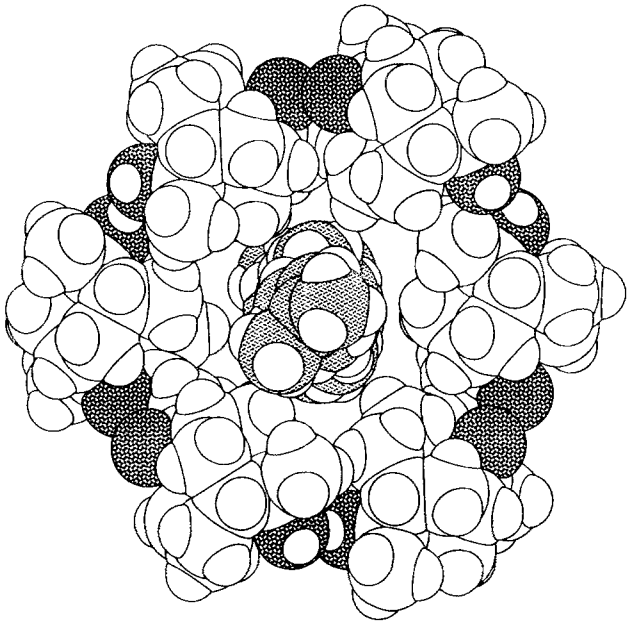

Fig. 4. Projection view along $c$ of the helical tubulate compound $(\mathbf{3})_3 \cdot (\text{squalene})_{0.23}$ showing the compact arrangement of the guest in one canal. Guest carbon atoms are shown using light stippling and host oxygen atoms using heavy stippling.

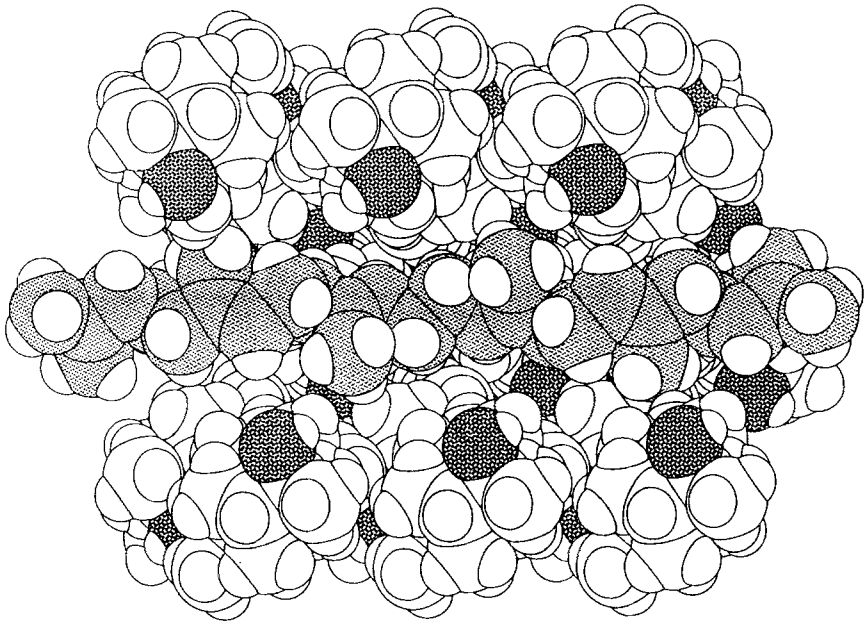

Fig. 5. Side view of one canal of Figure 4 with one column of diol host molecules removed to reveal the squalene guest. Carbon atoms of the squalene are stippled for clarity. Heavy stippling represents the oxygen atoms of the host.

TABLE V. Fractional coordinates for the non-hydrogen atoms of $(\mathbf{3})_3 \cdot (\text{squalene})^{a}_{0.23}$.

| | $x$ | $y$ | $z$ |
|---|---|---|---|
| O | -0.2371(1) | 0.3792(1) | 0.2285(2) |
| C(1) | 0.0035(1) | 0.3320(3) | 0.1667(0) |
| C(2) | -0.0992(2) | 0.3362(2) | 0.1145(3) |
| C(3) | -0.1420(2) | 0.3691(2) | 0.2919(2) |
| C(4) | -0.0495(2) | 0.4770(2) | 0.3891(2) |
| C(5) | 0.0660(2) | 0.4809(2) | 0.3917(2) |
| C(6) | -0.1895(2) | 0.2709(2) | 0.4352(3) |
| C(7) | -0.0429(2) | 0.5882(2) | 0.3341(4) |
| C(8) | -0.0479(3) | 0.6201(3) | 0.1499(7) |
| HO | -0.2806(22) | 0.3784(23) | 0.3385(32) |
| SQC(1) | 0.0369(12) | -0.0099(10) | -1.4979(40) |
| SQC(2) | 0.0028(4) | -0.0010(4) | -1.3119(7) |
| SQC(3) | -0.0017(8) | 0.0731(9) | -1.1731(18) |
| SQC(4) | -0.0387(19) | -0.0702(19) | -0.9545(45) |
| SQC(5) | 0.0503(10) | 0.0315(8) | -0.8369(35) |
| SQC(6) | 0.0484(4) | 0.0121(4) | -0.7298(8) |
| SQC(7) | 0.1069(8) | 0.0796(11) | -0.6123(18) |
| SQC(8) | 0.0961(24) | 0.0291(40) | -0.4066(47) |
| SQC(9) | 0.0040(9) | 0.0246(9) | -0.2873(37) |
| SQC(10) | 0.0414(4) | 0.0611(4) | -0.0665(8) |
| SQC(11) | -0.0333(5) | 0.0206(4) | 0.0631(7) |
| SQC(12) | 0.0000(7) | 0.0537(2) | 0.2718(4) |
| SQC(13) | -0.0286(4) | 0.0901(5) | -1.2660(9) |
| SQC(14) | -0.0294(4) | -0.1120(4) | -0.6732(13) |
| SQC(15) | 0.1657(6) | 0.1435(6) | -0.0161(8) |

[a] Squalene carbon atoms are prefixed by SQ.

the canal cross-section can vary significantly to enclose different sizes of guest. However there were only very small concomitant variations in the $c$ direction. Similar effects are observed here. For the benzene [5], ferrocene, and squalene inclusion compounds of diol **3**, the lengths of $a$, $b$ are 13.7404(8), 13.7480(6) and 13.677(1) Å, repectively. The corresponding values of $c$ are 7.0301(5), 7.0312(5) and 7.0533(9) Å. Thus while there must be a size limit for guest molecules, the lattice has a certain degree of flexibility in the $ab$ plane to accommodate bulkier guests.

Our work on the synthesis and development of the helical tubuland diol host family has been aimed at providing a series of host lattices with a significant range of canal dimensions [1, 2]. The present results demonstrate that, in addition to the smaller guests already reported [3, 4], guests with relatively large dimensions in

TABLE VI. Squalene dimensions in $(\mathbf{3})_3 \cdot (\text{squalene})_{0.23}$.

| | | | |
|---|---|---|---|
| *Bond Lengths* (Å) | | | |
| SQC(1)–SQC(2) | 1.53(4) | SQC(13)–SQC(2) | 1.55(5) |
| SQC(2)–SQC(3) | 1.34(4) | SQC(3)–SQC(4) | 1.51(4) |
| SQC(4)–SQC(5) | 1.56(4) | SQC(5)–SQC(6) | 1.51(3) |
| SQC(6)–SQC(7) | 1.37(3) | SQC(6)–SQC(14) | 1.47(4) |
| SQC(7)–SQC(8) | 1.54(4) | SQC(8)–SQC(9) | 1.54(4) |
| SQC(9)–SQC(10) | 1.51(3) | SQC(10)–SQC(11) | 1.34(3) |
| SQC(10)–SQC(15) | 1.54(5) | SQC(11)–SQC(12) | 1.50(4) |
| SQC(12)–SQC(12)[a] | 1.49(4) | | |
| *Bond Angles* (°) | | | |
| SQC(1)–SQC(2)–SQC(13) | 122(3) | SQC(1)–SQC(2)–SQC(3) | 120(2) |
| SQC(13)–SQC(2)–SQC(3) | 118(3) | SQC(2)–SQC(3)–SQC(4) | 117(2) |
| SQC(3)–SQC(4)–SQC(5) | 108(2) | SQC(4)–SQC(5)–SQC(6) | 118(2) |
| SQC(14)–SQC(6)–SQC(7) | 118(2) | SQC(6)–SQC(7)–SQC(8) | 116(2) |
| SQC(7)–SQC(8)–SQC(9) | 108(2) | SQC(8)–SQC(9)–SQC(10) | 108(2) |
| SQC(9)–SQC(10)–SQC(11) | 120(2) | SQC(9)–SQC(10)–SQC(15) | 121(2) |
| SQC(15)–SQC(10)–SQC(11) | 119(2) | SQC(10)–SQC(11)–SQC(12) | 117(2) |
| SQC(11)-SQC(12)-SQC(12)[a] | 109(2) | | |
| *Torsional Angles* (°) | | | |
| SQC(1)–SQC(2)–SQC(3)–SQC(4) | | 178(3) | |
| SQC(2)–SQC(3)–SQC(4)–SQC(5) | | -106(3) | |
| SQC(3)–SQC(4)–SQC(5)–SCQ(6) | | -119(2) | |
| SQC(4)–SQC(5)–SQC(6)–SQC(7) | | -156(2) | |
| SQC(5)–SQC(6)–SQC(7)–SQC(8) | | 177(2) | |
| SQC(6)–SQC(7)–SQC(8)–SQC(9) | | -95(3) | |
| SQC(7)–SQC(8)–SQC(9)–SQC(10) | | -110(2) | |
| SQC(8)–SQC(9)–SQC(10)–SQC(11) | | -139(2) | |
| SQC(9)–SQC(10)–SQC(11)–SQC(12) | | 179(2) | |
| SQC(10)–SQC(11)–SQC(12)–SQC(12)[a] | | -141(2) | |
| SQC(11)–SQC(12)–SQC(12)[a]–SQC(11)[a] | | -153(4) | |

[a] $x - y, -y, 2/3 - z$.

either cross-section or length can be accommodated within the large canals of the diol **3** lattice.

The material deposited comprises fractional coordinates of the hydrogen atoms, thermal parameters and structure factors.

## Acknowledgement

We thank the Australian Research Council for financial support of this work.

## References


1. R. Bishop and I. G. Dance: in *Inclusion Compounds*, J. L. Atwood, J. E. D. Davies and D. D. MacNicol, Eds.; Oxford University Press: Oxford, 1991; Vol. 4, Ch. 1, pp. 1–26.
2. R. Bishop and I. G. Dance: *Top. Curr. Chem.* **149**, 137 (1988).
3. A. T. Ung, R. Bishop, D. C. Craig, I. G. Dance and M. L. Scudder: *J. Chem. Soc., Perkin Trans. 2* 861 (1992).
4. A. T. Ung, R. Bishop, D. C. Craig, I. G. Dance and M. L. Scudder: *Struct. Chem.* **3**, 59 (1992).
5. I. G. Dance, R. Bishop, S. C. Hawkins, T. Lipari, M. L. Scudder and D. C. Craig: *J. Chem. Soc., Perkin Trans. 2* 1299 (1986).
6. I. G. Dance, R. Bishop and M. L. Scudder: *J. Chem. Soc., Perkin Trans. 2* 1309 (1986).
7. R. Bishop, I. G. Dance, S. C. Hawkins and M. L. Scudder: *J. Incl. Phenom.* **5**, 229 (1987).
8. R. M. Herath Banda, I. G. Dance, T. D. Bailey, D. C. Craig, and M. L. Scudder: *Inorg. Chem.* **28**, 1862 (1989).
9. P. Seiler and J. D. Dunitz: *Acta Crystallogr., Sect. B* **35**, 2020 (1979).
10. A. D. Rae: *RAELS*, A Comprehensive Constrained Least-Squares Refinement Program, University of New South Wales (1989).
11. InsightII, Version 2.1.0, Biosym Technologies, San Diego (1992).
12. J. Ernst, W. S. Sheldrick and J.-H. Fuhrhop: *Angew. Chem. Intl. Ed. Engl.* **15**, 778 (1976).
13. J. Ernst and J.-H. Fuhrhop: *Liebigs Ann. Chem.* 1635 (1979).
14. A. Freer, C. J. Gilmore, D. D. MacNicol and D. R. Wilson: *Tetrahedron Lett.* **21**, 1159 (1980).
15. G. Clec'h, G. Calvarin, J. F. Bérar and R. Kahn: *C. R. Acad. Sci., Ser. C* **286**, 315 (1978).
16. P. Seiler and J. D. Dunitz: *Acta Crystallogr., Sect. B* **35**, 1068 (1979).
17. F. Takusagawa and T. F. Koetzle: *Acta Crystallogr. Sect. B* **35**, 1074 (1979).
18. R. Clement, R. Claude and C. Mazieres: *J. Chem. Soc., Chem. Commun.* 654 (1974).
19. A. N. Nesmayanov, G. B. Shul'pin and M. I. Pybinskaya: *Dokl. Akad. Nauk SSSR* **221**, 624 (1975); *Chem. Abstr.* **83**, 58989j (1975).
20. E. Hough and D. G. Nicholson: *J. Chem. Soc., Dalton Trans.* 15 (1978).
21. A. Harada and S. Takahashi: *J. Chem. Soc., Chem. Commun.* 645 (1984); A. Harada, Y. Hu, S. Yamamoto and S. Takahashi: *J. Chem. Soc., Dalton Trans.* 729 (1988).
22. Y. Odagaki, K. Hirotsu, T. Higuchi, A. Harada and S. Takahashi: *J. Chem. Soc., Perkin Trans. I* 1230 (1990).
23. Z. Narankiewicz, A. L. Blumenfeld, V. L. Bondareva, I. R. Mamedyarova, M. N. Nefedova and V. I. Sokolov: *J. Incl. Phenom.* **11**, 233 (1991).
24. K. Miki, N. Kasai, H. Tsutsumi, M. Miyata and K. Takemoto: *J. Chem. Soc., Chem. Commun.* 545 (1987).
25. S. C. Hawkins, R. Bishop, D. C. Craig, I. G. Dance, A. D. Rae and M. L. Scudder: *J. Chem. Soc., Perkin Trans. 2*, in press.